22

# Adaptive Beamforming Algorithm Using a Pre-filtering System

Omar Abu-Ella[1] and Bashir El-Jabu[2]
[1]*Assistant Lecturer, Seventh October University,*
[2]*Associate Professor, Higher Industrial Institute, Misurata,*
*Libya*

## 1. Introduction

As depicted in Fig. 1, adaptive beamforming algorithms can be classified into two categories: non-blind adaptive algorithms and blind adaptive algorithms [1]. Non-blind adaptive algorithms rely on statistical knowledge about the transmitted signal in order to converge to a solution. This is typically accomplished through the use of a pilot training sequence sent over the channel to the receiver to help it identifying the desired user. On the other hand, blind adaptive algorithms do not require prior training, and hence they are referred to as "blind" algorithms. These algorithms attempt to extract salient characteristic of the transmitted signal in order to separate it from other users in the surrounding environment [2]. In this chapter we propose a technique that could be used with the blind or non blind algorithms to enhance their performance. This technique acts on the input signal vector **x**(k) as a band pass filter but in spatial domain, so it minimizes the noise and interference effects as a function of the Direction of Arrivals (DOAs).

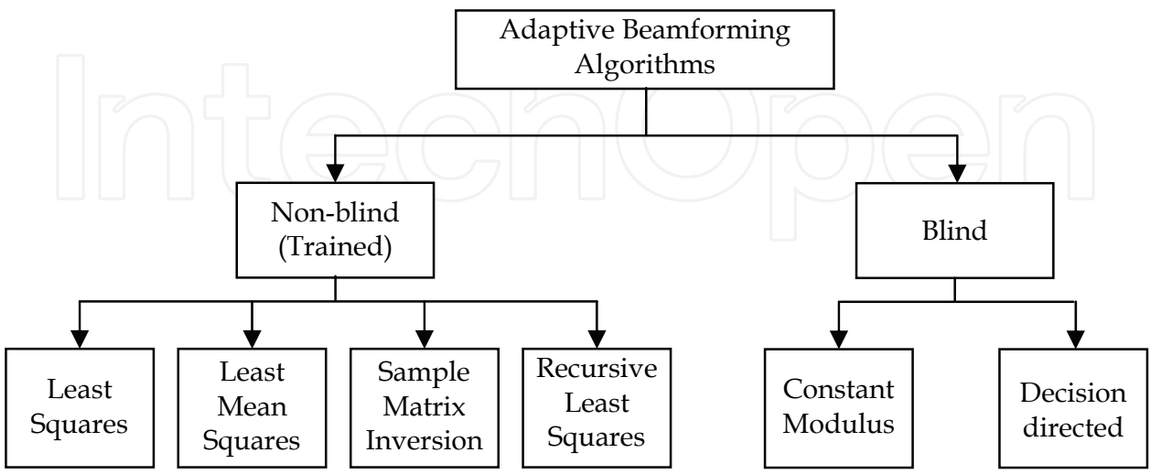


Fig. 1. General classifications of adaptive array algorithms

Source: Aerospace Technologies Advancements, Book edited by: Dr. Thawar T. Arif,
ISBN 978-953-7619-96-1, pp. 492, January 2010, INTECH, Croatia, downloaded from SCIYO.COM

## 2. Proposed hybrid adaptive beamforming technique

The proposed technique which introduced in [3] aims to increase the Signal-to-Interference and Noise Ratio (SINR) of the beamforming system by reducing the interference and noise effects on the desired user signal using filtering in spatial domain, or extracting the desired signal from the instantaneous input signal vector **x**(k) of the beamformer, as can be seen in Fig. 2. In this context, it is worth pointing out that in image processing, especially in image compressing techniques, one can find an abundance of techniques that can reconstruct the original image with acceptable performance, without using all transformation components, but rather using only the lower component coefficients of the image transform matrix [4]. We will exploit this fact with some modifications and employ it in the antenna array processing to obtain a new beamforming technique.

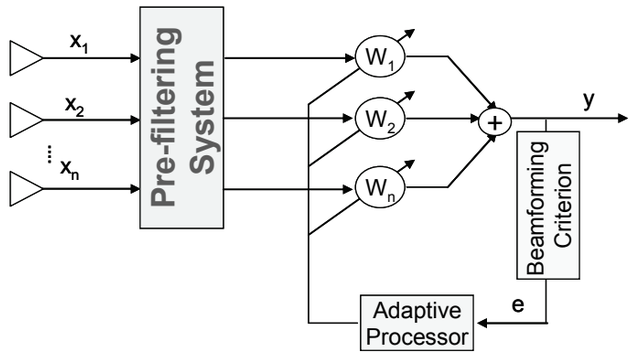


Fig. 2. Proposed blind adaptive beamformer with pre-filtering system

Since the interfering signals are in the same frequency band of the desired signal, we investigate representing them in another domain other than frequency domain so as to distinguish between the mixed signals that form the input signal. Therefore, the proposed technique is based on the idea that the desired and interfering signals arrive at the antenna array from different directions. Thus, we exploit these differences between arriving signals. The distinction can be obtained by converting the input signal to the spectrum of the spatial domain (this domain is the sine of the direction of arrival, or $\sin\theta$ domain). The desired signal can be extracted from the input system signals simply by making a band-pass filter in the spectrum of the spatial domain, i.e., in the $\sin\theta$ spectrum. This filtering process is shown in Fig. 3, and can be explained generally as follows:

- The original input signal is passed through a Fast Fourier Transform (FFT) stage to obtain its coefficients in the spectrum domain.
- The Most Significant Coefficient (MSC) of the transformed signal is selected. This is ranked as the largest sample of the transformed desired signal.
- The most significant coefficient is placed at its rank in the M zeros element vector (zero padding).
- The Inverse Fast Fourier Transform (IFFT) is applied to the filtered vector of the previous step to reconstruct an alternative input signal that contains a reduced amount of interference and noise.
- The reconstructed data vector is used as input signal to the adaptive beamforming system.

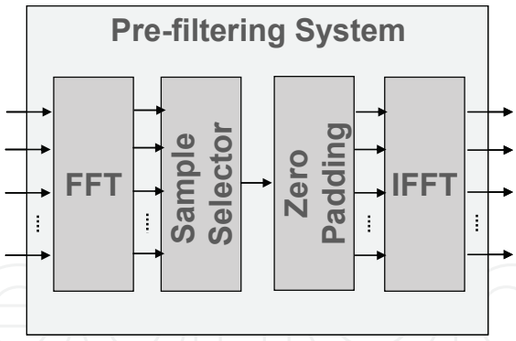


Fig. 3. Pre-filtering system

Mathematically, assuming that the narrow band array propagation vector for the $\theta$ direction of arrival is given by

$$\mathbf{a}(\theta) = e^{-j2\pi\frac{d}{\lambda}\sin\theta(m-1)},\ m = 1,2,\cdots,M \tag{1}$$

where $M$ is the number of array elements, $d$ is the spacing distance between any two adjacent elements, and $\lambda$ is the wavelength of the operating carrier frequency. Applying the FFT on the array propagation (Equation 1) gives

$$\begin{aligned}\mathbf{A}(\Theta) &= FFT\left(\mathbf{a}(\theta)\right)\\ &= \frac{1}{M}\sum_{m=1}^{M} e^{-j2\pi\frac{d}{\lambda}\sin\theta(m-1)} e^{-j2\pi K(m-1)/M}\\ &= \frac{1}{M}\sum_{m=1}^{M} e^{-j2\pi\left(\frac{d}{\lambda}\sin\theta(m-1)+\frac{K}{M}(m-1)\right)}\end{aligned} \tag{2}$$

Let $d = \lambda/2$, then

$$\begin{aligned}\mathbf{A}(\Theta) &= \frac{1}{M}\sum_{m=1}^{M} e^{-j2\pi\left(\frac{K}{M}+\frac{\sin\theta}{2}\right)(m-1)}\\ &= \frac{1}{M}\frac{e^{j\pi(2K+M\sin\theta)/M} - e^{-j2\pi(2K+M\sin\theta)(M-1)/M}}{e^{j\pi(2K+M\sin\theta)/M} - 1}\\ &= \frac{1}{M}\left\{\frac{e^{j\pi\left(\frac{2K+\sin\theta}{M}\right)\left(\frac{3-2M}{2}\right)}\left[e^{j\pi\left(\frac{2K+M\sin\theta}{M}\right)\left(M-\frac{1}{2}\right)} - e^{-j\pi\left(\frac{2K+M\sin\theta}{M}\right)\left(M-\frac{1}{2}\right)}\right]}{e^{j\pi\left(\frac{2K+\sin\theta}{2M}\right)}\left[e^{j\pi\left(\frac{2K+M\sin\theta}{2M}\right)} - e^{-j\pi\left(\frac{2K+M\sin\theta}{2M}\right)}\right]}\right\}\\ &= e^{-j\pi\left(\frac{2K+\sin\theta}{M}\right)(M-1)}\left[\frac{\sin\left(\pi\left(\frac{2K+M\sin\theta}{M}\right)\left(M-\frac{1}{2}\right)\right)}{M\sin\left(\pi\left(\frac{2K+M\sin\theta}{2M}\right)\right)}\right]\end{aligned} \tag{3}$$

By differentiating Equation (3) and equating the result to zero, the following formula gives the index $K_{MSC}$ (or the order) of the most significant coefficient as a function of the direction of arrival $\theta$ and the number of array elements $M$

$$K_{MSC} = \left[ -\frac{1}{2} \left( \frac{M \left[ 2\pi M \sin\theta - \pi \sin\theta + j2 \tanh^{-1} \left( \frac{M - \frac{1}{2}}{M - 1} \right) \right]}{\pi(2M-1)} \right) \right]_{\text{int}} \tag{4}$$

where $[x]_{\text{int}}$ means the integer part of $x$.

Since the index $K_{MSC}$ must be a real integer, the formula in Equation (4) is modified to take the form

$$K_{MSC} = \underset{M}{\text{mod}} \left\{ 1 + M \left[ -\frac{1}{2} \left( \frac{M(2\pi M \sin\theta - \pi \sin\theta)}{\pi(2M-1)} \right) \right]_{\text{int}} \right\} \tag{5}$$

where $\underset{M}{\text{mod}}$ is the modulus notation, performed on M points.

Equation (5) can be simplified to

$$K_{MSC} = \underset{M}{\text{mod}} \left( \left[ 1 - \tfrac{1}{2} M \sin\theta \right] \right) \tag{6}$$

To illustrate the idea of the pre-filtering system consider, as an example, an array of 4 elements, with desired DOA = –45˚and signal sample $s_d$= - 0.0035 - 0.1000i. Then, from Equation (1) the array propagation factor at the desired direction is

$$\mathbf{a}(\theta_d) = \begin{bmatrix} 0.9990 - 0.0000\text{i} \\ -0.6049 + 0.7958\text{i} \\ -0.2663 - 0.9623\text{i} \\ 0.9280 + 0.3715\text{i} \end{bmatrix}$$

Thus, the desired signal vector $\mathbf{s} = s_d \mathbf{a}(\theta_d)$ is given by

$$\mathbf{s} = \begin{bmatrix} -0.0035 - 0.0999\text{i} \\ 0.0817 + 0.0577\text{i} \\ -0.0953 + 0.0300\text{i} \\ 0.0339 - 0.0941\text{i} \end{bmatrix}$$

And assuming that there is an undesired signal vector u, such that:

$$\mathbf{u} = \begin{bmatrix} -0.0241 - 0.7054\text{i} \\ -0.7078 + 0.0253\text{i} \\ 0.0239 + 0.7065\text{i} \\ 0.7069 - 0.0256\text{i} \end{bmatrix}$$

Thus, by adding the weighted desired and the desired signals the total input signal is given as:

$$\mathbf{x} = \begin{bmatrix} -0.0276 - 0.8053i \\ -0.6261 + 0.0830i \\ -0.0714 + 0.7365i \\ 0.7408 - 0.1197i \end{bmatrix}$$

By passing this input data vector through the FFT stage, we get the following transform coefficients vector

$$\mathbf{X} = \begin{bmatrix} 0.0156 - 0.1055i \\ 0.2465 - 0.1749i \\ -0.2137 - 0.0322i \\ -0.1589 - 2.9087i \end{bmatrix}$$

Appling Equation (6) on the given DOA and the number of array elements we find that the most significant coefficient is the second coefficient. Replacing the other coefficients by zeros, we get the following vector

$$\mathbf{X}_z \begin{bmatrix} 0 \\ 0.2465 - 0.1749i \\ 0 \\ 0 \end{bmatrix}$$

Now, applying the IFFT on the zero padded vector we get the reconstructed input vector as follows

$$\tilde{\mathbf{x}} = \begin{bmatrix} 0.0616 - 0.0437i \\ 0.0437 + 0.0616i \\ -0.0616 + 0.0437i \\ -0.0437 - 0.0616i \end{bmatrix}$$

To take advantage of the pre-filtering technique to reduce the mean square error (MSE), we determine the fluctuations of the original input data vector $\tilde{\mathbf{x}}$ and the reconstructed input data vector $\mathbf{x}$ from the desired signal vector $\mathbf{s}$

$$\mathbf{s} - \mathbf{x} = \begin{bmatrix} 0.0241 + 0.7054i \\ 0.7078 - 0.0253i \\ -0.0239 - 0.7065i \\ -0.7069 + 0.0256i \end{bmatrix}$$

$$\mathbf{s} - \tilde{\mathbf{x}} = \begin{bmatrix} -0.0652 - 0.0562i \\ 0.0379 - 0.0039i \\ -0.0338 - 0.0137i \\ 0.0776 - 0.0324i \end{bmatrix}$$

MSE of the conventional technique = $20\log\left(\left|\mathbf{s}-\mathbf{x}\right|\right)$ = 9.0306 dBv

MSE of the proposed technique = $20\log\left(\left|\mathbf{s}-\tilde{\mathbf{x}}\right|\right)$ = -12.2258 dBv.

It is clear that the proposed technique reduces the MSE in this example by more than 21 dB; this improvement is significant in communications systems.

As explained in the general steps shown in Fig. 4, the output of the pre-filtering stage is applied as an input to the beamforming algorithms. The flowchart of the whole process using the constant modulus algorithm CMA(1,2) is as indicated in the figure. Other algorithms (other than the CMA) can also be used.

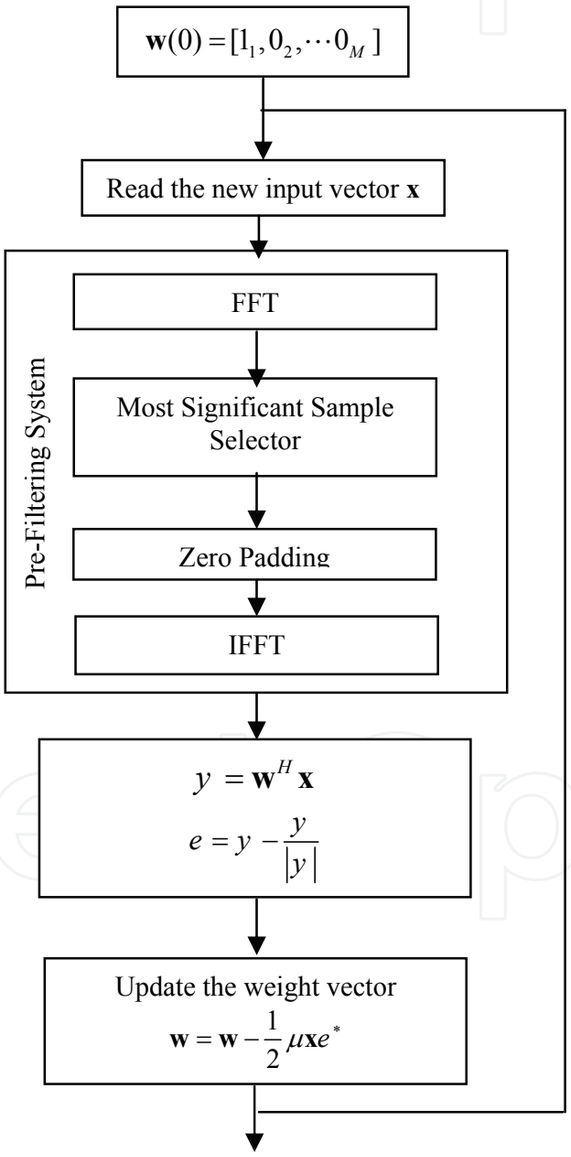


Fig. 4. Flowchart of the proposed hybrid technique

## 3. Quadratic diagram and the SIR improvement in the beamformer input signal using the proposed hybrid technique

The quadratic (i.e. the complex plane) diagram of the input signal vector to the beamformer system is represented in Fig.5, where $\mathbf{s}_i$ , $\mathbf{u}_i$ and $\mathbf{x}_i$ represent, respectively, the desired, undesired and the total input signal on the ith element of the array . For clarity, only the angles of $\mathbf{s}_1$ , $\mathbf{u}_1$ , $\mathbf{x}_1$ are shown.

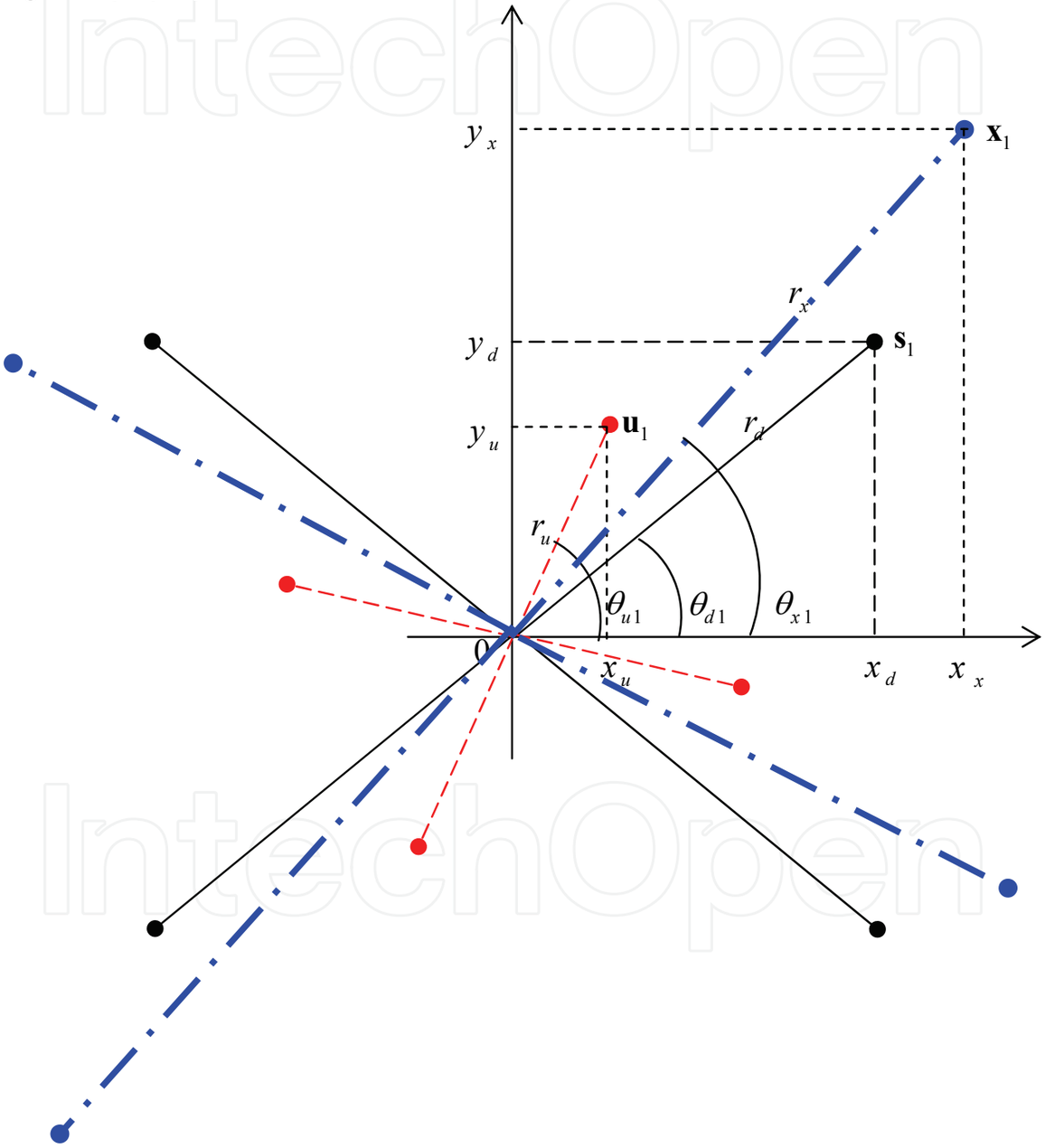


Fig. 5. The desired, interfering and the total input signal vectors in the quadratic plane

The desired signal vector can be represented as

$$\mathbf{s} = s\mathbf{a}(\theta_d) \tag{7}$$

where $\mathbf{a}(\theta_d)$ is the array propagation vector corresponding to the desired direction and it is given as,

$$\mathbf{a}(\theta_d) = e^{-j\frac{2\pi}{\lambda}(m-1)d\sin\theta_d}, m = 1,2,\cdots,M$$

and $s = r_d e^{j\phi_d}$ is the desired signal sample. Equation (7) can be put in the form

$$\mathbf{s} = r_d e^{j\phi_d} e^{-j\frac{2\pi}{\lambda}(m-1)d\sin\theta_d} \tag{8}$$

Assuming $d = \lambda/2$, the desired signal vector can be written in the form

$$\mathbf{s} = r_d e^{j(\phi_d - \pi(m-1)\sin\theta_d)} \tag{9}$$

The complex rectangular coordinates of the vectors can be expressed as

$$x_d = r_d \cos\left(\phi_d - \pi\left(m-1\right)\sin\theta_d\right) \tag{10a}$$

$$y_d = r_d \sin\left(\phi_d - \pi\left(m-1\right)\sin\theta_d\right)\ m = 1,2,\cdots,M \tag{10b}$$

It is clear that the resulting signal is an array containing vectors with a constant magnitude $r_d$, and each vector has a specific phase $\phi_d(m) = -\pi(m-1)\sin\theta_d$, $m = 1,2,\cdots,M$. Similarly, the undesirable signal vector can be put in the form

$$\mathbf{u} = r_u e^{j(\phi_u - \pi(m-1)\sin\theta_u)} \tag{11}$$

the complex rectangular coordinates of which can be expressed as

$$x_u = r_u \cos\left(\phi_u - \pi\left(m-1\right)\sin\theta_u\right)$$

$$y_u = r_u \sin\left(\phi_u - \pi\left(m-1\right)\sin\theta_u\right) \tag{12}$$

In case of interference, the total received signal can be put as

$$\mathbf{x} = \mathbf{s} + \mathbf{u} \tag{13}$$

$$\mathbf{x} = r_d e^{j(\phi_d - \pi(m-1)\sin\theta_d)} + r_u e^{j(\phi_u - \pi(m-1)\sin\theta_u)} \tag{14}$$

for which, the complex rectangular coordinates may be written as:

$$x_x = r_d \cos\left(\phi_d - \pi\left(m-1\right)\sin\theta_d\right) + r_u \cos\left(\phi_u - \pi\left(m-1\right)\sin\theta_u\right)$$

$$y_x = r_d \sin\left(\phi_d - \pi\left(m-1\right)\sin\theta_d\right) + r_u \sin\left(\phi_u - \pi\left(m-1\right)\sin\theta_u\right) \tag{15}$$

The resulting overall vector magnitude can be obtained as follows

$$\begin{aligned} r_x &= \sqrt{{x_x}^2 + {y_x}^2} \\ &= \sqrt{\left(x_d + x_u\right)^2 + \left(y_d + y_u\right)^2} \\ &= \sqrt{\left({x_d}^2 + {y_d}^2\right) + \left({x_u}^2 + {y_u}^2\right) + 2\left(x_d x_u + y_d y_u\right)} \\ &= \sqrt{\left({r_d}^2 + {r_u}^2\right) + 2 r_d r_u \psi} \end{aligned} \tag{16}$$

where

$$\begin{aligned} \psi = &\cos\left(\phi_d - \pi\left(m-1\right)\sin\theta_d\right)\cos\left(\phi_u - \pi\left(m-1\right)\sin\theta_u\right) \\ &+ \sin\left(\phi_d - \pi\left(m-1\right)\sin\theta_d\right)\sin\left(\phi_u - \pi\left(m-1\right)\sin\theta_u\right) \end{aligned} \tag{17}$$

is the variation in the total signal magnitude (desired and undesired signals) caused by the interference (undesirable signals). Here, $\psi(m)$ is not a constant value for all values of $m$ except when $\theta_d$ and $\theta_u$ are equal; in this case the proposed technique will not improve SIR; but generally most of beamforming algorithms fail in this case. Since we have assumed in this chapter that the interfering signal arrive at a direction different from the desired signal direction, $r_x(m)$ can not to be a constant value, i.e., the total input signal vector $\mathbf{x}(m)$ will appear scattered in the complex plane.

To show the Signal-to-Interference Ratio (SIR) improvement in the input signal vector using the proposed hybrid beamforming technique we determine the gained signal-to-interference ratio in the reconstructed signal vector using the pre-filtering technique of the hybrid beamforming system. Assuming a linear system, the total input signal vector $x(m)$ is the sum of the desired signal **s**(m) and the undesired one $\mathbf{u}(m)$ –i.e.-

$$\mathbf{x}(m) = \mathbf{s}(m) + \mathbf{u}(m) \tag{18}$$

Similarly, for the reconstructed input data vector $\tilde{x}(m)$ ,

$$\tilde{\mathbf{x}}(m) = \tilde{\mathbf{s}}(m) + \tilde{\mathbf{u}}(m) \tag{19}$$

where $\tilde{\mathbf{s}}(m)$ , and $\tilde{\mathbf{u}}(m)$ are the desired and undesired reconstructed signals vector respectively. To generalize the procedure, we will assume that an arbitrary signal sample $v = re^{j\phi}$ arrives to the array at $\theta$ direction. Therefore, the array signal vector of this signal will be in the form

$$\mathbf{v}(m) = re^{j\phi}e^{-j\pi\sin\theta(m-1)}, \quad m = 1, 2, \cdots, M \tag{20}$$

The fast Fourier transform of the resulting signal vector $\mathbf{v}(m)$ is

$$\begin{aligned} \mathbf{V}(k) &= FFT\left[\mathbf{v}(m)\right] \\ &= \sum_{m=1}^{M} \mathbf{v}(m) \cdot e^{j2\pi(k-1)(m-1)/M} \\ &= \sum_{m=1}^{M} re^{j\phi} \cdot e^{j2\pi(k-1)(m-1)/M} \end{aligned}$$

$$= re^{j\phi} \cdot e^{-j\frac{\pi}{2}\left[M\sin\theta+2(k-1)\right](M+1)/M} \cdot \left[\frac{\sin\left(\frac{\pi}{2}\left[M\sin\theta+2(k-1)\right]\right)}{\sin\left(\frac{\pi}{2}\left[M\sin\theta+2(k-1)\right]/M\right)}\right] \tag{21}$$

Now, the value of the specific $k$th coefficient from the transformed signal vector $\mathbf{V}(k)$ can be calculated. This coefficient will be selected to reconstruct the signal vector $\tilde{\mathbf{v}}(m)$ . Substituting for the $k$th index in Equation (6) into Equation (21) gives the value of the most significant coefficient as

$$\mathbf{V}(k_{MSC}) = re^{j\phi} \cdot e^{-j\frac{\pi M}{2}\left[\sin\theta-\sin\theta_d\right](M+1)/M} \cdot \left[\frac{\sin\left(\frac{-\pi M}{2}\left[\sin\theta-\sin\theta_d\right]\right)}{\sin\left(\frac{\pi}{2}\left[\sin\theta-\sin\theta_d\right]\right)}\right] \tag{22}$$

This value will be put in a zeros vector in the rank of the $k_{MSC}$ so that we can express the resulting signal vector as

$$\mathbf{V}(k_{MSC}) = re^{j\phi} \cdot e^{-j\frac{\pi M}{2}\left[\sin\theta-\sin\theta_d\right](M+1)/M} \cdot \left[\frac{\sin\left(\frac{-\pi M}{2}\left[\sin\theta-\sin\theta_d\right]\right)}{\sin\left(\frac{\pi}{2}\left[\sin\theta-\sin\theta_d\right]\right)}\right] \cdot \delta(k-k_{MSC}), \quad k=1,2,\cdots M \tag{23}$$

where

$$\delta(k-k_{MSC}) = \begin{cases} 1, k = k_{MSC} \\ 0, \text{elsewhere} \end{cases}$$

The reconstructed signal vector can be obtained by applying inverse Fourier transformation to Equation (23) as follows

$$\tilde{\mathbf{v}}(m) = \frac{1}{M}\sum_{k=1}^{M}\mathbf{V}(k_{MSC})e^{j2\pi(k-1)(m-1)/M}$$

$$= \frac{1}{M}\mathbf{V}(k_{MSC})e^{-j\pi\sin\theta_d(m-1)}$$

$$= re^{j\phi}e^{-j\pi\sin\theta_d(m-1)}e^{-j\frac{\pi M}{2}\left[\sin\theta-\sin\theta_d\right](M+1)/M} \cdot \frac{1}{M}\left[\frac{\sin\left(\frac{-\pi M}{2}\left[\sin\theta-\sin\theta_d\right]\right)}{\sin\left(\frac{\pi}{2}\left[\sin\theta-\sin\theta_d\right]\right)}\right] \tag{24a}$$

Therefore, we can put the signals in the form

$$\tilde{\mathbf{v}} = G_1(r,\phi,\theta)\cdot G_2(\theta) \tag{24b}$$

where

$$G_1(r,\phi,\theta) = re^{j\phi}\cdot e^{-j\pi\sin\theta_d(m-1)}\cdot e^{-j\frac{\pi M}{2}[\sin\theta-\sin\theta_d](M+1)/M} \tag{24c}$$

It is clear from Equation (24 c) that the magnitude of $G_1$ equals the signal magnitude $r$ and

$$G_2(\theta) = \frac{1}{M}\left[\frac{\sin\left(\frac{-\pi M}{2}\left[\sin\theta-\sin\theta_d\right]\right)}{\sin\left(\frac{\pi}{2}\left[\sin\theta-\sin\theta_d\right]\right)}\right] \tag{24d}$$

The variation of $G_2$ as a function of $\theta$ is shown in Fig. 6 from which it is clear that its value equal unit only if and only $\theta = \theta_d$. Fig. 7 shows the effects of the gains on the magnitude of the desired, undesired and the total input signal.
In Fig. 7, it is assumed that $r_d > r_u$ without loss of generality.
Note that, in case of $\tilde{\mathbf{s}}$

$$G_1(r_d,\phi_d,\theta_d) = r_d e^{j\phi_d} e^{-j\pi\sin\theta_d(m-1)} \tag{25a}$$

and from Equation (2d)

$$G_2(\theta_d) = 1 \tag{25b}$$

Note that, in case of $\tilde{\mathbf{u}}$

$$G_1(r_u,\phi_u,\theta_u) = r_u e^{j\phi_u}\cdot e^{-j\pi\sin\theta_d(m-1)}\cdot e^{-j\frac{\pi M}{2}[\sin\theta_u-\sin\theta_d](M+1)/M} \tag{25c}$$

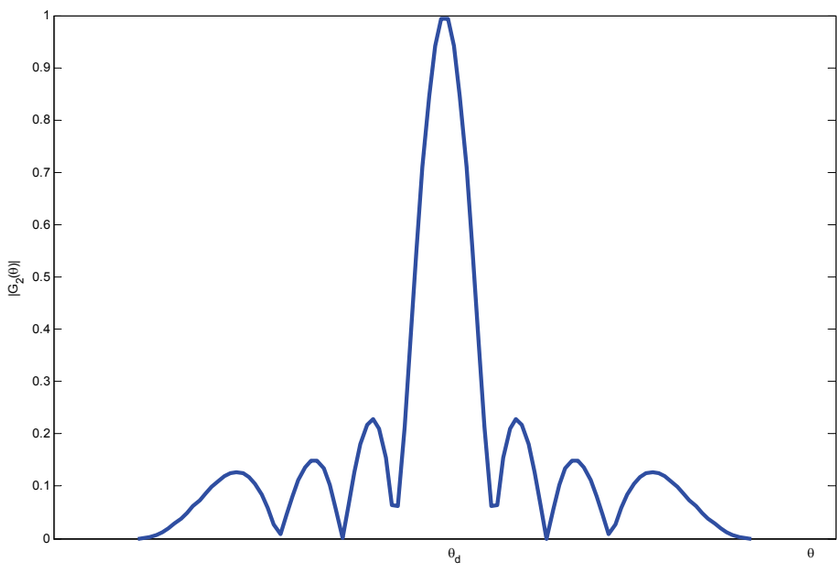


Fig. 6. Magnitude of $G_2$ versus DOA

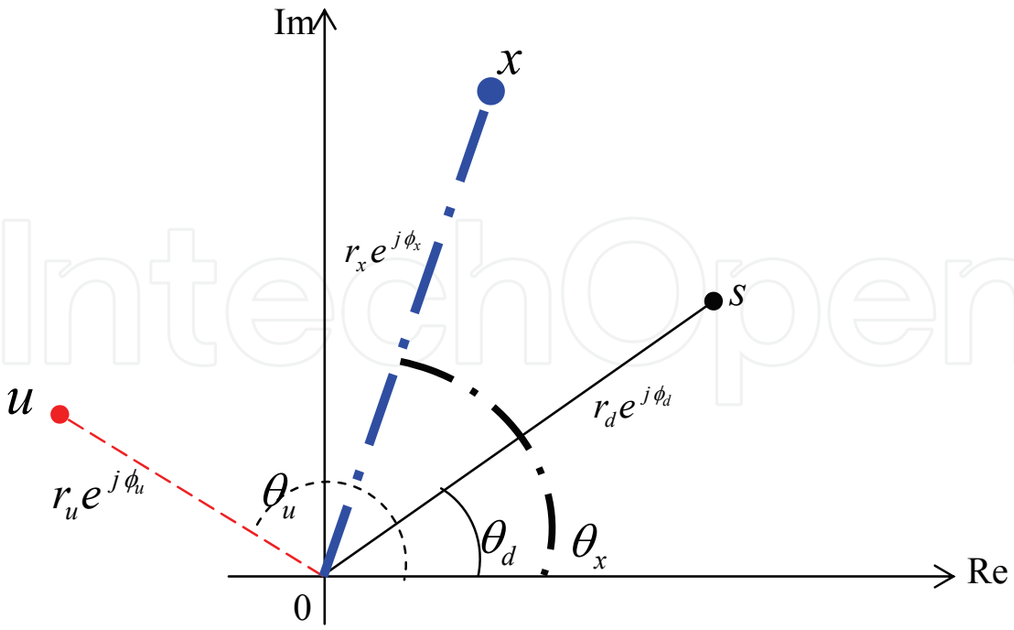


Fig. 7. Desired, interference and the total input signal in the quadratic plane

and

$$G_2(\theta_u) = \frac{1}{M}\left[\frac{\sin\left(\frac{-\pi M}{2}\left[\sin\theta_u - \sin\theta_d\right]\right)}{\sin\left(\frac{\pi}{2}\left[\sin\theta_u - \sin\theta_d\right]\right)}\right] \tag{25d}$$

Note that in case of the desired signal (i.e. $\theta = \theta_d$) $G_2$ will be equals one i.e. the maximum value. However, in case of the undesired signal (i.e. $\theta = \theta_u$) $G_2$ will be attenuated i.e. will be less than one.

The overall reconstructed input signal vector $\tilde{\mathbf{x}}(m)$, which consists of the desired signal vector and attenuated interfering signal vector can be given by

$$\tilde{\mathbf{s}} = G_1(r_d, \phi_d, \theta_d) \cdot G_2(\theta_d)$$

and

$$\tilde{\mathbf{u}} = G_1(r_u, \phi_u, \theta_u) \cdot G_2(\theta_u) \tag{26}$$

Substituting Equation (26) into Equation (19) gives

$$\begin{aligned}\tilde{\mathbf{x}}(m) &= r_d e^{j\phi_d} e^{-j\pi \sin\theta_d (m-1)} \\ &+ r_u e^{j\phi_u} e^{-j\pi \sin\theta_d (m-1)} e^{-j\frac{\pi M}{2}\left[\sin\theta_u - \sin\theta_d\right](M+1)/M} \\ &\cdot \frac{1}{M}\left[\frac{\sin\left(\frac{-\pi M}{2}\left[\sin\theta_u - \sin\theta_d\right]\right)}{\sin\left(\frac{\pi}{2}\left[\sin\theta_u - \sin\theta_d\right]\right)}\right]\end{aligned} \tag{27}$$

Note that the overall reconstructed $\tilde{\mathbf{x}}(m)$ (overall reconstructed signal on the $m$th element) has a constant magnitude, because its derivative with respect to m is zero (i.e. $\frac{d}{dm}\left(\left|\tilde{\mathbf{x}}(m)\right|\right)=0$), which means that the hybrid technique eliminates the magnitude fluctuation which is described in Equations (16) and (17).

As a result, we can evaluate the signal-to-interference ratio SIR improvement in the reconstructed input vector $\tilde{\mathbf{x}}(m)$. Since the magnitude of the desired signal vector stays constant without any attenuation and the interfering signal vector magnitude is decreased by the factor $\left|\frac{1}{M}\left[\frac{\sin\left(-\pi M/2\left[\sin\theta_u-\sin\theta_d\right]\right)}{\sin\left(\pi/2\left[\sin\theta_u-\sin\theta_d\right]\right)}\right]\right|$, therefore, the maximum possible gained $SIR_G$ in dB can be expressed as

$$SIR_G = 20\log\left\{\left|\frac{M\sin\left(\frac{\pi}{2}\left[\sin\theta_u-\sin\theta_d\right]\right)}{\sin\left(\frac{-\pi M}{2}\left[\sin\theta_u-\sin\theta_d\right]\right)}\right|\right\} dB \tag{28}$$

A simulation setup will be used to show the improvements in the reconstructed input signal vector. Fig. 8 shows a quadratic diagram representation of a desired signal, arriving at DOA of 60˚, an interfering signal with arbitrary DOA of 40˚, the original received signal without using the pre-filtering technique, and the reconstructed signal after the pre-filtering process. From these results, one can observe that the reconstructed input data vector is closer to the desired signal than the original received input vector which is scattered by the interference effects. For this reason, the pre-filtering process is performed directly before the beamforming process in the proposed hybrid algorithm. This will help the beamformer in extracting the desired signal in easier and faster way.

Fig. 9 illustrates the quadratic diagram of a similar scenario but with the desired signal arriving at DOA of 45˚ and 6 undesired signals arriving at DOAs of (19˚, 60˚, 120˚, 240˚, 300˚, 341˚) with respect to the DOA of the desired signal. In this figure, one can observe the extensively scattering of the compound interfering signal which causes the scattering of the original input data vector. However, the same figure shows that the reconstructed input signal is not scattered and nearer to the desired signal. Thus, pre-filtering effectively reduces the noise and interfering.

In summary, the pre-filtering technique generates a new input data signal with lower undesired signal than the original one. This reduction is obtained previously by taking the most significant coefficient of the desired signal (and ignoring the other coefficients) (similar to bandpass filtering). To see the possibility of reducing the undesired signal by discarding the most significant coefficient of the undesired signal (similar to band reject filtering), the same scenario is used in Fig. 8 gave the results shown in Fig. 10 which illustrates lower performance.

## 4. Simulation results

This section compares the performance of the proposed hybrid adaptive algorithms with some of conventional adaptive beamforming algorithms. The factors used for this comparison are:

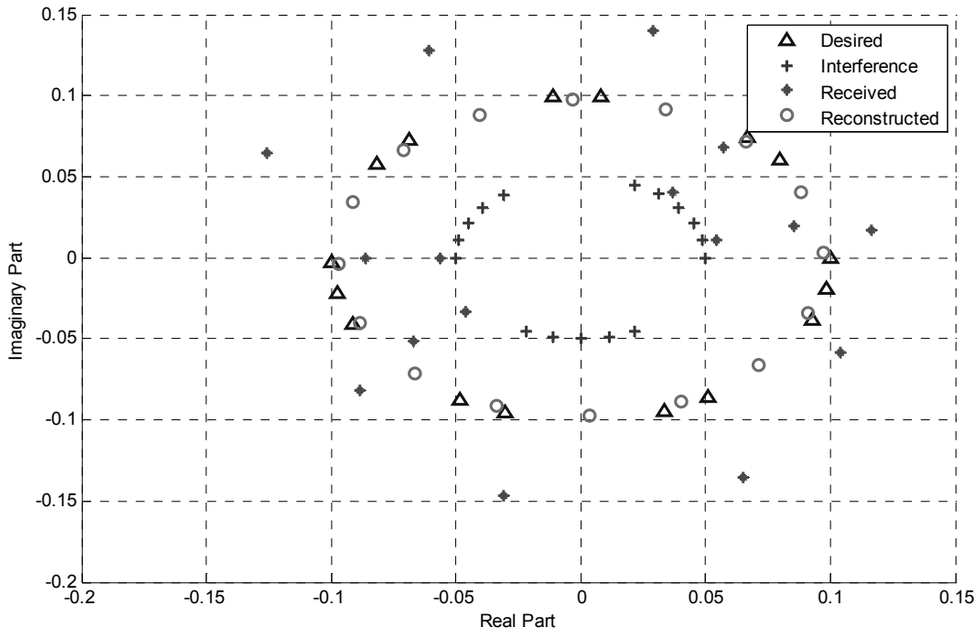


Fig. 8. Quadratic diagram in case of single interferer signal

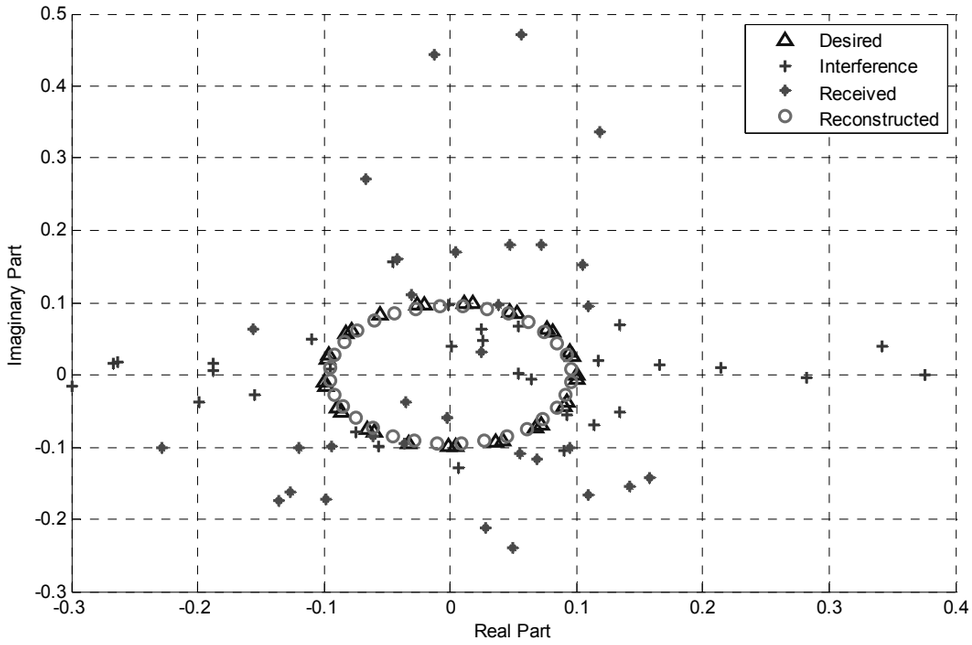


Fig. 9. Quadratic diagram in case of multiple interferer signals

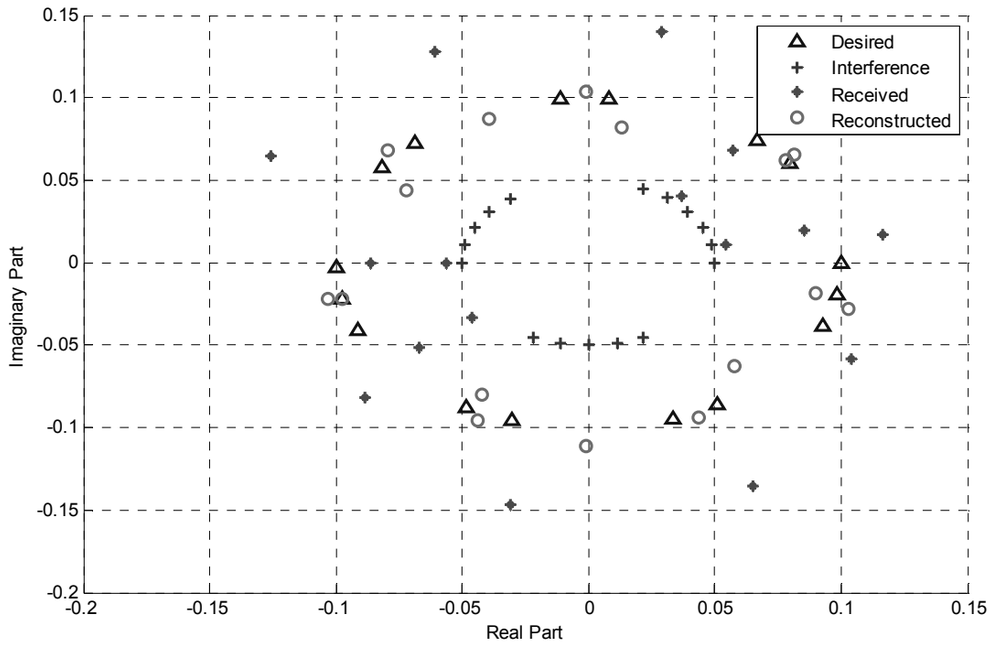


Fig. 10. Quadratic diagrams (complex plane) in case of discarding the interferer signal

- Beam Pattern Characteristics (Beam gain in small angular separation between desired and undesired signals).
- Resulting Signal-to-Interference Ratio SIR.
- Bit Error Rate (BER) behavior with Respect to SINR.
- System Capacity (Number of user in the system).
- The Outage Probability of the System.
- Computational Complexity.
- Convergence Speed.
- Tracking performances

In each case, simulation environment parameters are assumed to realize the system in the case. Overall simulation environments are written using MATLAB code.

### 4.1 Beam pattern performance

The array response to the signal with direction of arrival $\theta$ is given by [5]

$$G(\theta) = \sum_{i=1}^{M} w_i^* e^{-j\frac{2\pi}{\lambda}(i-1)d\sin\theta} \tag{29}$$

where $w_i$ is the $i$th value of the weight vector. This array response, $G(\theta)$, can also be represented in a vector form as

$$G(\theta) = \mathbf{w}^H \mathbf{a}(\theta) \tag{30}$$

where **w** is the weight vector and $H$ is the Hermitian notation. The beam pattern $G_{BP}$ defined as the magnitude of $G(\theta)$ has the form

$$G_{BP}(\theta) = \left| \mathbf{w}^H \mathbf{a}(\theta) \right| \tag{31}$$

Initially, a simulation is carried out assuming arrival direction of the desired signal at 60˚ interfering signal arrives from 50˚(small separation angle and equal power of the desired signal, which represents a tight condition) and the initial weights vector is taken as the first column of the identity matrix, i.e. $\mathbf{w}(0) = [1, 0, 0, \cdots, 0_M]^T$ . The results obtained after 1000 iterations, using an adaptive array system with eight antennas. The beam pattern obtained for the conventional Constant Modulus Algorithm (CMA), which is considered as one of the most efficient blind algorithms and the proposed technique. A comparison between these two results is displayed in Fig.11. It is clear that the maximum gain of the main lobe directed toward the desired direction for the proposed hybrid technique is greater than that for the conventional CMA by about 2 dB, and the minimum gain (null) at undesired direction for the proposed technique is less than that for the conventional CMA by 7 dB (better performance). This means that the proposed hybrid algorithm is more efficient in forming the beam pattern. The results are as displayed in Fig. 12 from which it is clear that the directivity of the hybrid algorithm is higher than that of the conventional one, i.e., the former is more capable in distinguishing between neighboring users (a serious problem for conventional blind adaptive beamforming algorithm).

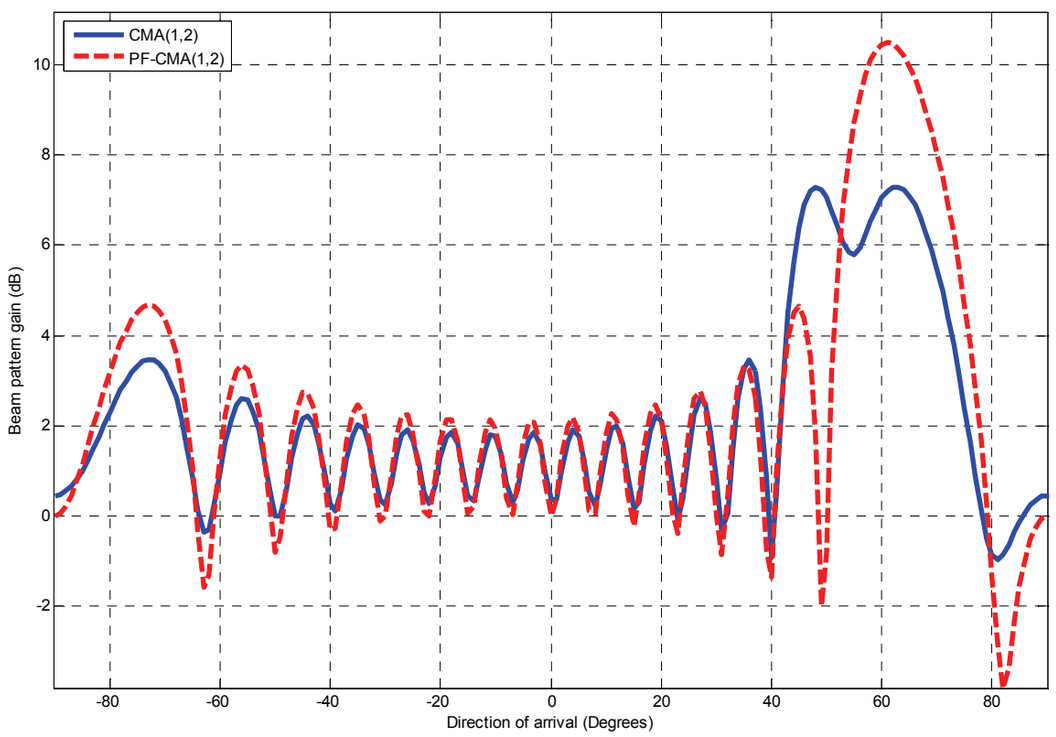


Fig. 11. Beam patterns of CMA and hybrid technique in (dB)

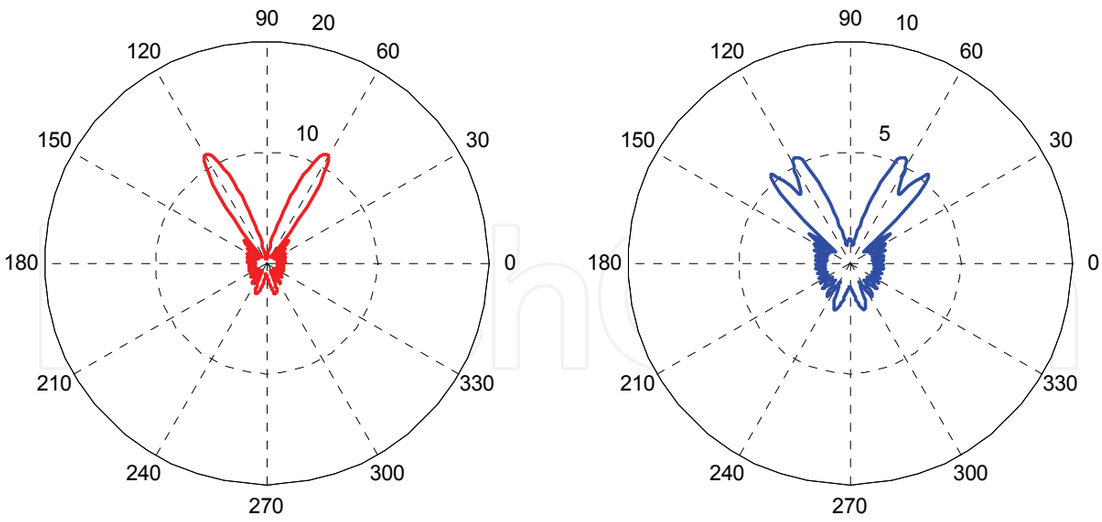


(a) Polar beam pattern of hybrid technique (b) Polar beam pattern of CMA(1, 2)

Fig. 12. Polar beam patterns of CMA and hybrid technique for small angular separation between desired and interfering DOAs

### 4.2 Signal-to-Interference Ratio (SIR) performance and power budget

The SIR for adaptive array can be written to have the form

$$SIR = \frac{\mathbf{w}^H s_d{}^2 \mathbf{a}(\theta_d)\mathbf{a}^H(\theta_d)\mathbf{w}}{\mathbf{w}^H \mathbf{R}_I \mathbf{w}} \tag{32}$$

where $\mathbf{a}(\theta_d)$ is the array propagation vector at the desired direction of arrival, $s_d$ is the desired signal sample, and $\mathbf{R}_I$ is the covariance matrix of the interference signal.

The simulation is carried out under the same previous conditions, but with lower noise level. Fig. 13 shows the results. The steady state of the hybrid technique is at about 23 dB while that of the conventional algorithm is less than 6 dB (improvement of more than 17 dB in favor of the proposed technique). The SIR for both algorithms is evaluated as a function of interfering DOA assuming the desired user is at 0˚. Fig. 14 indicates a better performance for the hybrid technique in most of the time.

To obtain the power budget in this tight case, i.e., at a smaller angular separation of 10 degrees, we determined the ratio between the gain beam pattern at desired direction, $G_d$, and the maximum possible gain $G_{\max}$, i.e. $G_d/G_{\max}$. This ratio is 11/16 for the hybrid CMA technique and 5/16 for the conventional CMA, another advantage of the proposed technique (Gain of the power budget more than 3 dB).

### 4.3 BER behavior with respect to SINR

This part studies the effects of the proposed technique on the required SINR to achieve a specific bit error rate. Through out this chapter the required BER is assumed to be $10^{-8}$ because of simulation considerations, since a BER of $10^{-k}$ needs $10^{(k+1)}$ samples for the simulation results to lie within a confidence interval of 90% [2]. The conventional CMA

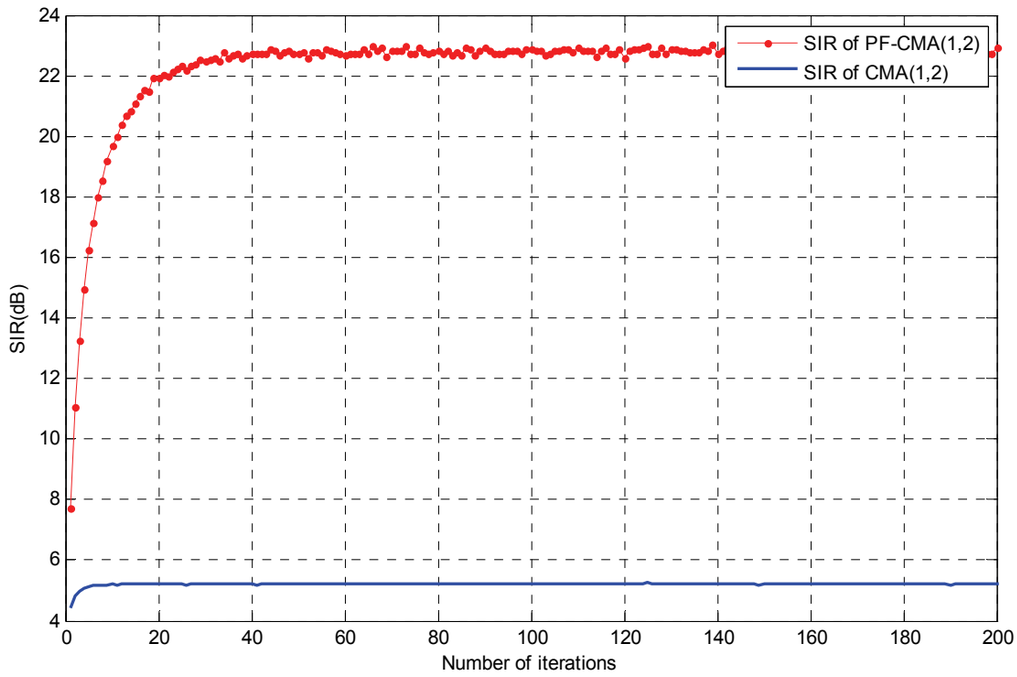


Fig. 13. SIR versus the number of iterations for the conventional CMA and hybrid technique

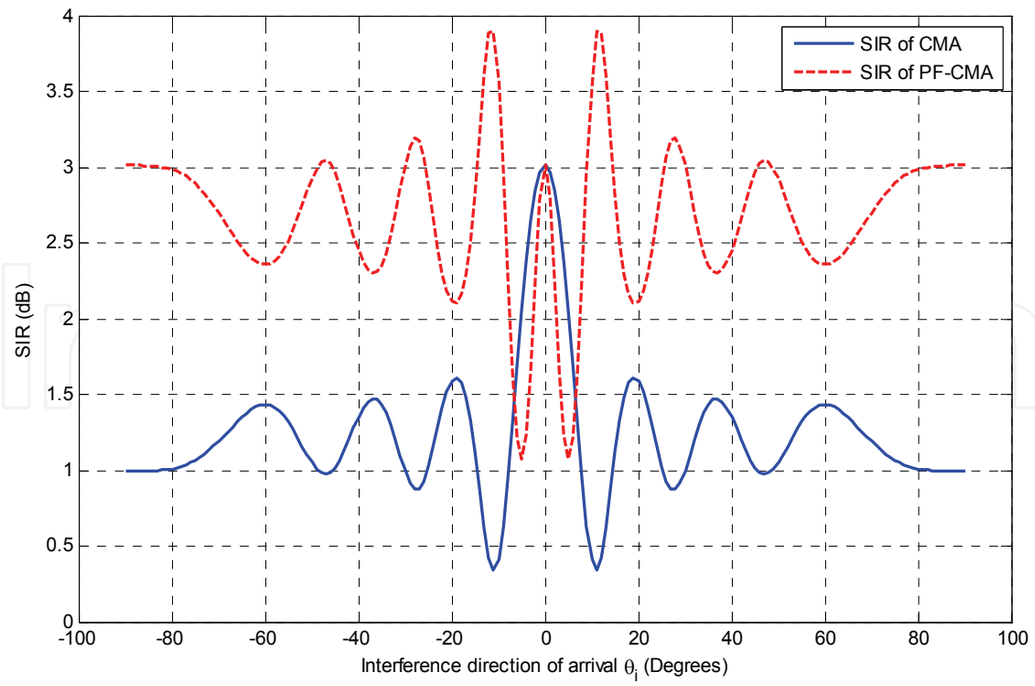


Fig. 14. SIR variations against interference direction of arrival for desired direction of arrival = 0˚

algorithm will be used as a reference. The results shown in Fig. 15 are obtained using an array receiving a desired signal at 0˚ and 6 interfering signals arriving at 19˚, 60˚, 120˚, 240˚, 300˚ and 341˚. The array uses 4 elements. These curves show that in case of SNR = 6 dB, the proposed hybrid technique needs -12.7 dB SINR to achieve $10^{-8}$ BER while the conventional CMA algorithm needs -2.7 dB to achieve the same BER (a difference of 10 dB in favor of the proposed technique). When the SNR is changed to 20 dB the difference becomes 12 dB.

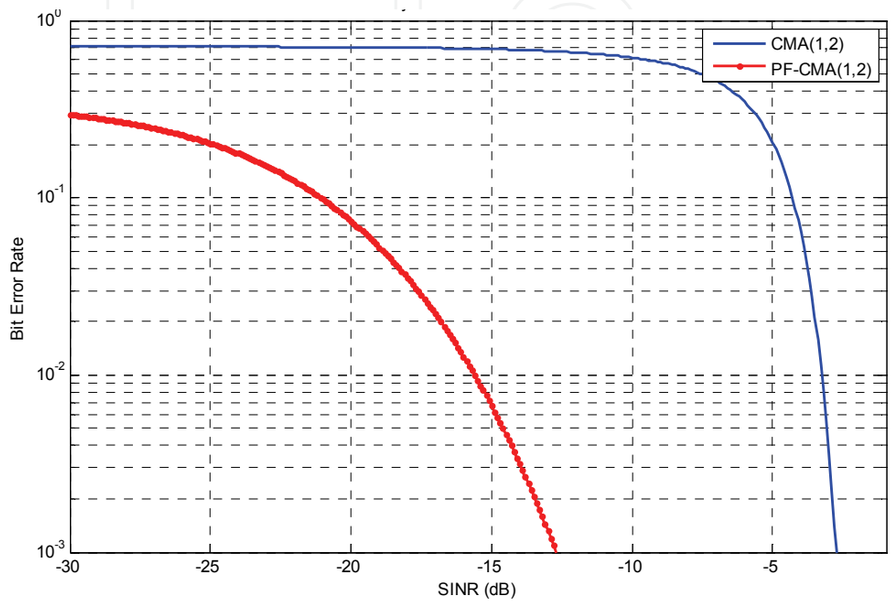


(a) SNR = 6dB

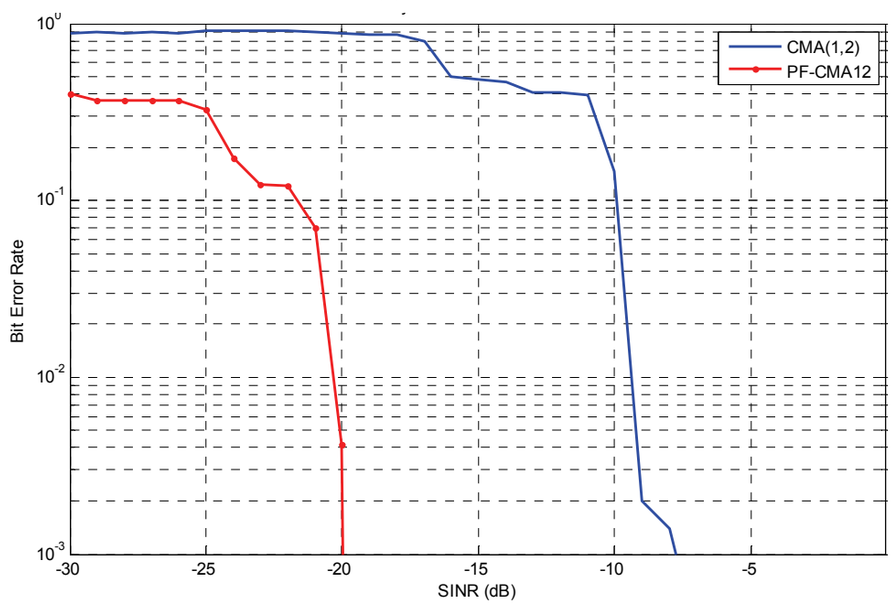


(b) SNR = 20dB

Fig. 15. BER versus SINR using CMA, hybrid technique, using 4-antenna array

### 4.4 System capacity

Beamforming often affects system capacity. Here, effect of the proposed technique on the capacity of cellular CDMA system is considered. System capacity (in terms of the number of users M) can be determined using [7]

$$M = \frac{\left(\frac{E_b}{I_o}\right)\left(\frac{R_b}{B_c}\right)+1}{(1+\gamma)\left(\frac{E_b}{I_o}\right)\left(\frac{R_b}{B_c}\right)} \tag{33}$$

where $E_b$ is the energy per bit, $I_o$ is the interference power spectral density (PSD) in Watts/Hertz, $R_b$ is the message data rate in bits per second, $B_c$ is the radio channel bandwidth in Hertz, where $B_c >> R_b$, and

$$\gamma = \frac{\sum_{j=1}^{J} G_{I_j}}{G_d} \tag{34}$$

is the inverse of the total SIR experienced by the mobile in the cell under considerations from the cochannel cells assuming one mobile per cochannel cell, $G_d$ is the desired beam gain evaluated at direction $\theta_d$, $G_{Ij}$ is the beam gain of the $j$th interfering cell evaluated at $\theta_i$. The aim of this proposed hybrid technique is to suppress the $\gamma$ value by decreasing the interference beam gain at $\theta_i$ direction. The factor $\gamma$ is evaluated by simulating the beamforming system with 4- and 8-element array antenna, in environment with 20 dB SNR assuming each interfering user generates interference power equal to the desired user power. A CDMA cellular system is assumed with service bit rate of 8000 and 32000 bps for each user, and with chip rate of 4 Mcps. The results are displayed in Fig. 16. The results shows that for the case of 8000bps rate the systems capacities for $E_b/I_o$ = -6dB are 213 and 228 users for the hybrid system using 4- and 8-element array respectively whereas the conventional system capacity are 80 and 89 users for 4 and 8 elements array system respectively. Thus, the proposed algorithm increases the system capacity by 1.5 folds comparing with the conventional system capacity. The same trend applies for the case of 32000 bps service bit rate as shown in Fig. 16 (b).

### 4.5 The outage probability

Here, the effect of the proposed technique on the outage probability for both up link and down link will be consider.

#### 4.5.1 Outage probability of the down-link system

The performance of the system can be expressed in terms of the outage probability, i.e., the probability that the bit error rate (BER) exceeds a certain threshold required BER, ($BER_{\max}$), normally$10^{-8}$, i.e.

$$P_o = \Pr\left(BER > BER_{\max}\right) \tag{35}$$

The outage probability can be defined as the probability that the SIR falls below minimum required SIR [6]. In cellular CDMA the system outage probability could be determined by the following [7]

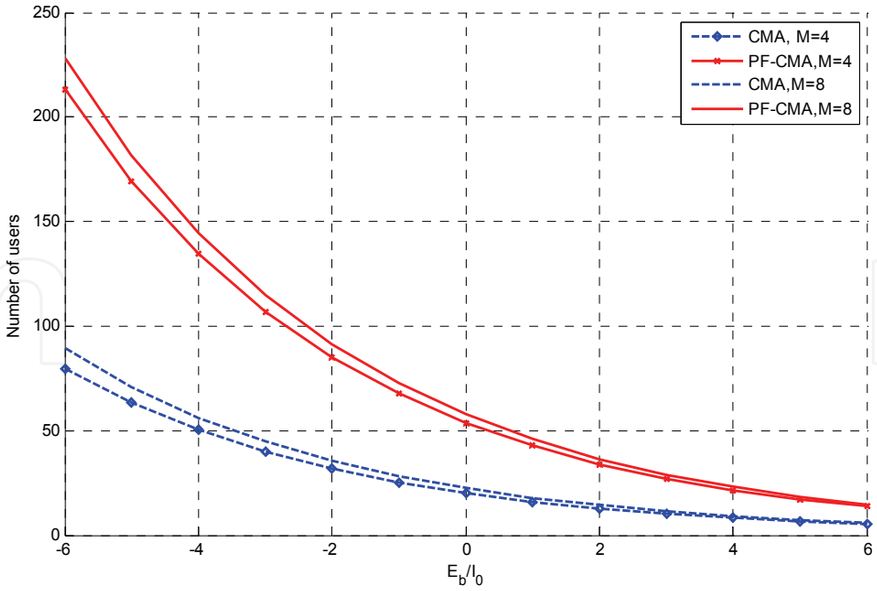


(a) Service bit rate =8000bps

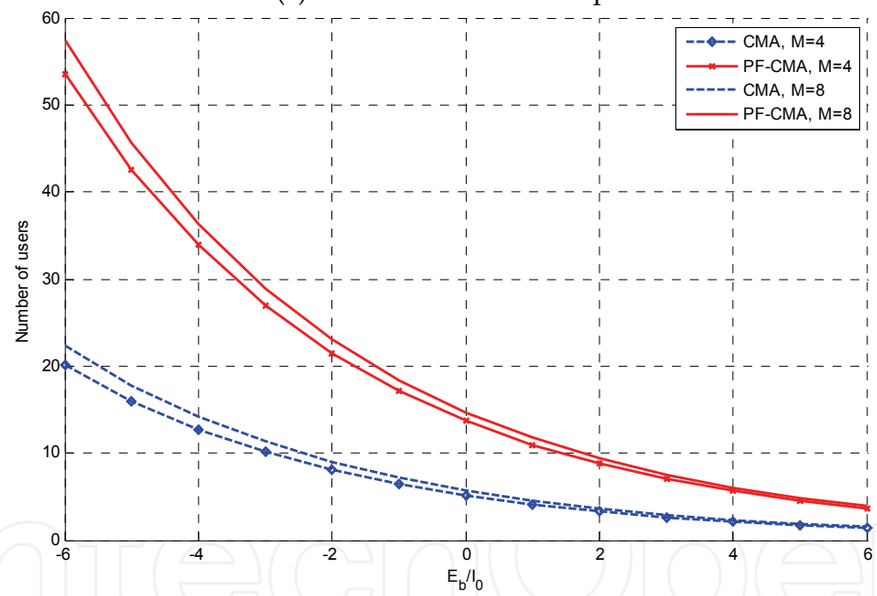


(b) Service bit rate =32000bps

Fig. 16. Number of users versus Eb/Io

$$p_o = Q\left(\frac{\chi - E\left[\frac{I_{out}}{S}\right]}{\frac{M}{G_P}\sqrt{\mathrm{var}\left[\frac{I_{out}}{S}\right]}}\right) \tag{36}$$

where $\chi = \frac{1}{\sigma_{req}} - \frac{I_{in}}{S} - \frac{\eta}{S}$, $E\left[I_{out}/S\right]$ is the ratio of the intercellular interference-to-signal ratio, $\sigma_{req}$ is the required SINR for the BER to be less than $BER_{\max}$, $M$ is the number of

users, $G_P$ is the processing gain, $\frac{\eta}{S}$ is the ratio of received thermal noise to user signal power, and

$$E\left[\frac{I_{out}}{S}\right] = \frac{(M+1)}{G_P} E[\gamma] = \frac{(M+1)}{G_P} \sum_{\substack{j=1 \\ j \neq k}}^{J} E\left[\frac{G(\theta_j)}{G(\theta_k)}\right] \tag{37}$$

where $E[\gamma]$ is the intercellular interference factor. Therefore, the outage probability will be given as

$$P_o = Q\left(\frac{\frac{1}{\sigma_{req}} - \frac{M+1}{G_P}(1+E[\gamma]) - \frac{\eta}{S}}{\frac{M}{G_P}\sqrt{\text{var}[\frac{I_{out}}{S}]}}\right) \tag{38}$$

The system with seven cells (desired one and six interfering using 8-element array system), which is represented in Fig. 17, is used to simulate the down-link of the cellular system in this section. The results of this simulation model are tabulated in Table 1.
Now, assuming M>>1, and using the simulation results in Table 1 we can expressed the outage probability using CMA(1,2) (conventional algorithm) for 8-element array system as follows

$$p_o = Q\left(\frac{\frac{1}{\sigma_{req}} - \frac{M\,7.7026}{G_P} - \frac{\eta}{s}}{\frac{M\,0.4520}{G_P}}\right) \tag{39}$$

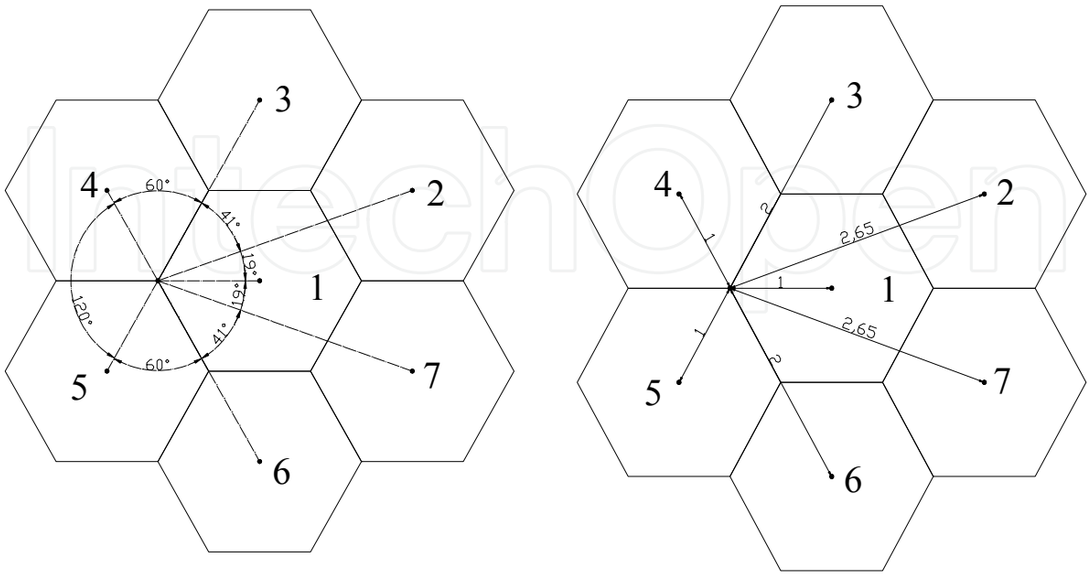


Fig. 17. Down-link cellular system with seven cells

| Technique | Item | Cell number (j) | | | | | | |
|---|---|---|---|---|---|---|---|---|
| | | 1 | 2 | 3 | 4 | 5 | 6 | 7 |
| CMA(1,2) | $G(\theta_j)$ | 1.8304 | 1.5027 | 2.3538 | 2.2899 | 2.3533 | 2.3457 | 1.4232 |
| | $G(\theta_j)/G(\theta_1)$ | 1.0000 | 0.8209 | 1.2859 | 1.2510 | 1.2857 | 1.2815 | 0.7775 |
| Hybrid Technique | $G(\theta_j)$ | 9.8264 | 1.5895 | 1.0812 | 0.9990 | 1.0812 | 1.0098 | 1.1439 |
| | $G(\theta_j)/G(\theta_1)$ | 1.0000 | 0.1618 | 0.1100 | 0.1017 | 0.1100 | 0.1028 | 0.1164 |

Table 1. Down-link beam gains at different directions of arrival

while that of the proposed technique is given by

$$p_o = Q\left(\frac{\frac{1}{\sigma_{req}} - \frac{M1.7027}{G_P} - \frac{\eta}{s}}{\frac{M0.2214}{G_P}}\right) \tag{40}$$

The results of Equation (39) and (40) are displayed in Fig. 18 for SNR = 0 dB and 20 dB. From this figure, it is clear that the hybrid technique decreases the outage probability of the system. This decrease will help in increasing the number of users that can be accommodated in the system (System Capacity). As an example, assuming that the acceptable outage probability is 1% and SNR = 0 dB, the system capacity will be 40 and 86 users for the conventional and hybrid system respectively, in case of 4-element array, and 45 and 108 users in case of 8-element array. Therefore, doubling the array size improves the system capacity by 11% and 26% for the conventional and hybrid systems respectively. In case of SNR = 20dB, the system capacity will be 45 and 95 users for the conventional and hybrid system respectively, in case of 4-element array, and 50 and 120 users in case of 8 elements array. Therefore, doubling the array size, again improves the system capacity by 11% and 26% for the conventional and hybrid systems respectively.

### 4.5.2 The outage probability of the up-link system

To check up-link performance improvement using the hybrid technique, we simulate the uplink cellular system shown in Fig. 19 using 6 interferer sources distributed uniformly around a central base station with a single desired user communicates with this station. We assumed that the interference sources located outside of the central base station cell. For simplicity, we assumed the distance of each interferer from the base station is double that of the desired user. The results of this simulation model are tabulated in Table 2.

Using Equation (38) and Table 2, the outage probability of the up-link cellular system using 16-element array for the conventional technique given by

$$p_o = Q\left(\frac{\frac{1}{\sigma_{req}} - \frac{M6.9501}{G_P} - \frac{\eta}{s}}{\frac{M0.0303}{G_P}}\right) \tag{41}$$

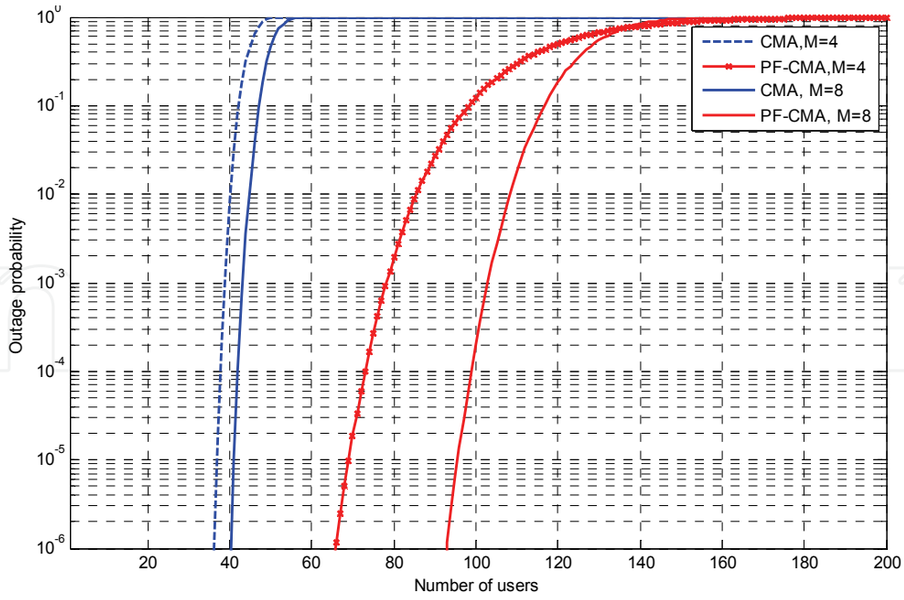


SNR= 0dB

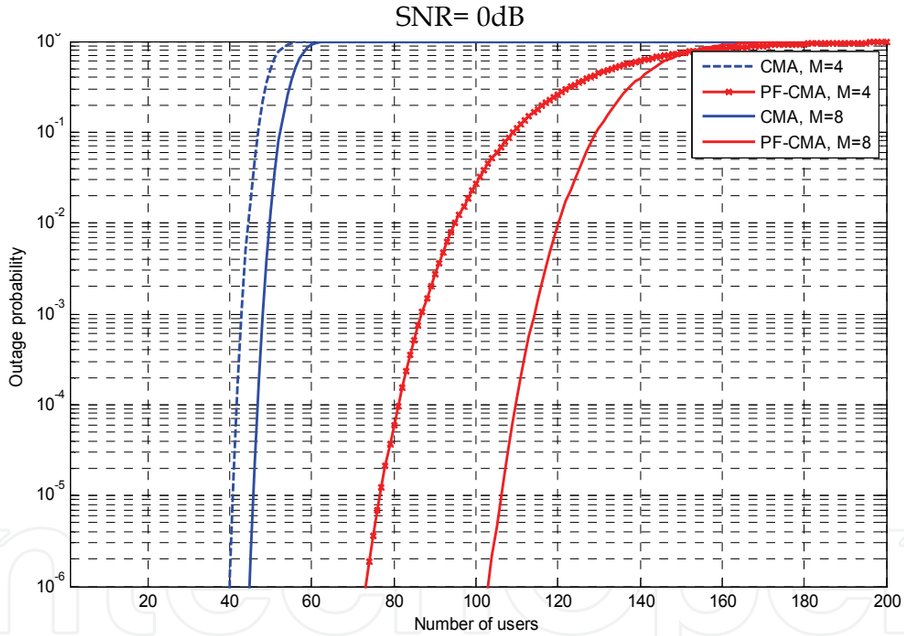


(b) SNR= 20dB

Fig. 18. The outage probability of cellular down link system with 4- and 8-element array while that of 16-element array for the propose hybrid technique is

$$p_o = Q\left(\frac{\frac{1}{\sigma_{req}} - \frac{M3.4715}{G_P} - \frac{\eta}{s}}{\frac{M0.1202}{G_P}}\right) \tag{42}$$

| Technique | Item | Cell number (j) | | | | | | |
|---|---|---|---|---|---|---|---|---|
| | | 1 | 2 | 3 | 4 | 5 | 6 | 7 |
| CMA(1,2) | $G(\theta_j)$ | 2.4981 | 2.4392 | 2.4998 | 2.4981 | 2.4967 | 2.4998 | 2.4394 |
| | $G(\theta_j)/G(\theta_1)$ | 1.0000 | 0.9764 | 1.0007 | 1.0000 | 0.9995 | 1.0007 | 0.9765 |
| Hybrid Technique | $G(\theta_j)$ | 10.000 | 0.9167 | 1.0000 | 1.0000 | 1.0000 | 1.0000 | 1.2663 |
| | $G(\theta_j)/G(\theta_1)$ | 1.0000 | 0.0917 | 0.1000 | 0.1000 | 0.1000 | 0.1000 | 0.1266 |

Table 2. Up-link beam gains at different directions of arrival

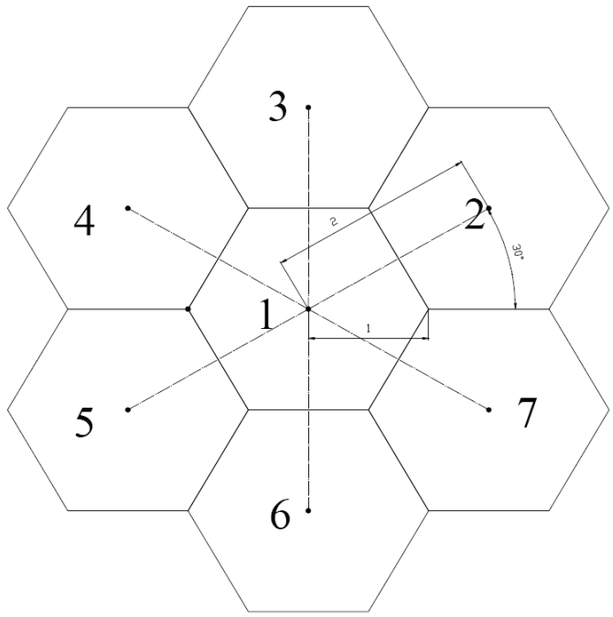


Fig. 19. Up-link cellular system with seven cells

The results are as shown in Fig.20 It is clear that the hybrid technique decreases the outage probability of the system. This decrease will help in increasing the number of users that can be accommodated in the system (System Capacity). As an example, assuming that the acceptable outage probability is 1% and SNR = 0dB, the system capacity will be 28 and 59 users for the conventional and hybrid system respectively, in case of 8-element array, and 34 and 67 users in case of 16-element array. Therefore, doubling the array size improves the system capacity by 21% and 14% for the conventional and hybrid systems respectively. In case of SNR = 20dB, the system capacity will be 31 and 65 users for the conventional and hybrid system respectively, in case of 8 elements array, and 37 and 75 users in case of 16 elements array. Therefore, doubling the array size, improves the system capacity by 19% and 15% for the conventional and hybrid systems respectively. Here we can observe that the capacity improvement percentage of the conventional algorithm is slightly greater than the improvement percentage of the overall hybrid technique, but in all of above cases the hybrid system capacity is greater.

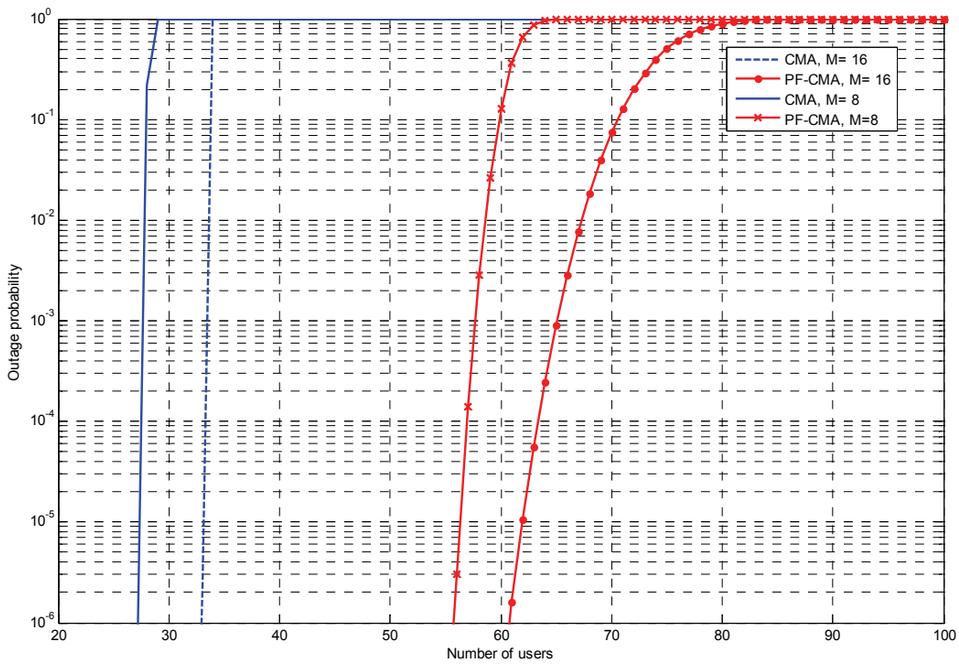


(a) SNR=0 dB

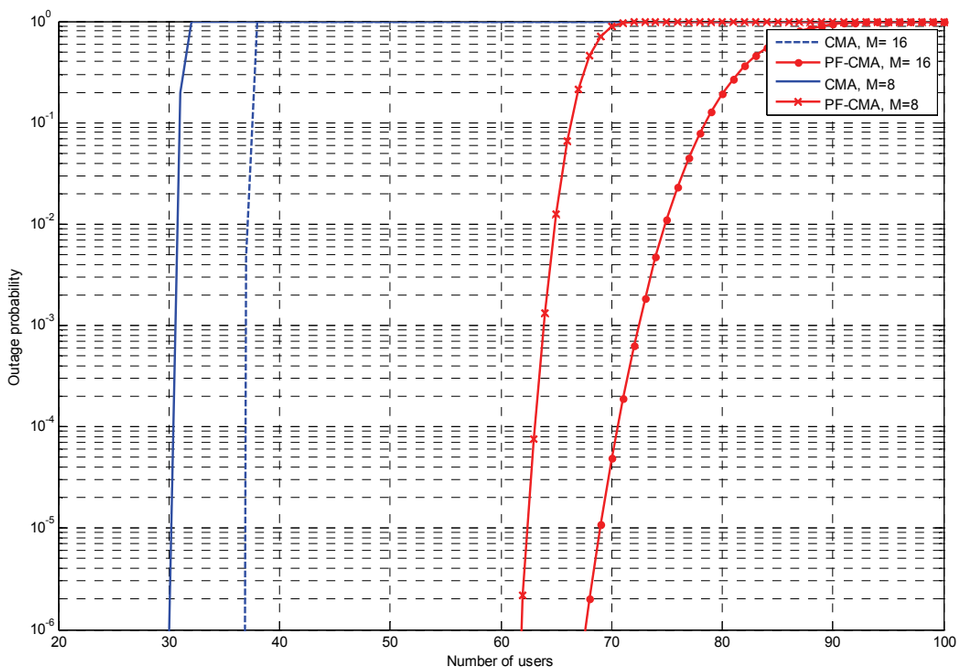


(b) SNR=20dB

Fig. 20. Outage probability of up-link system with 8- and 16- element array

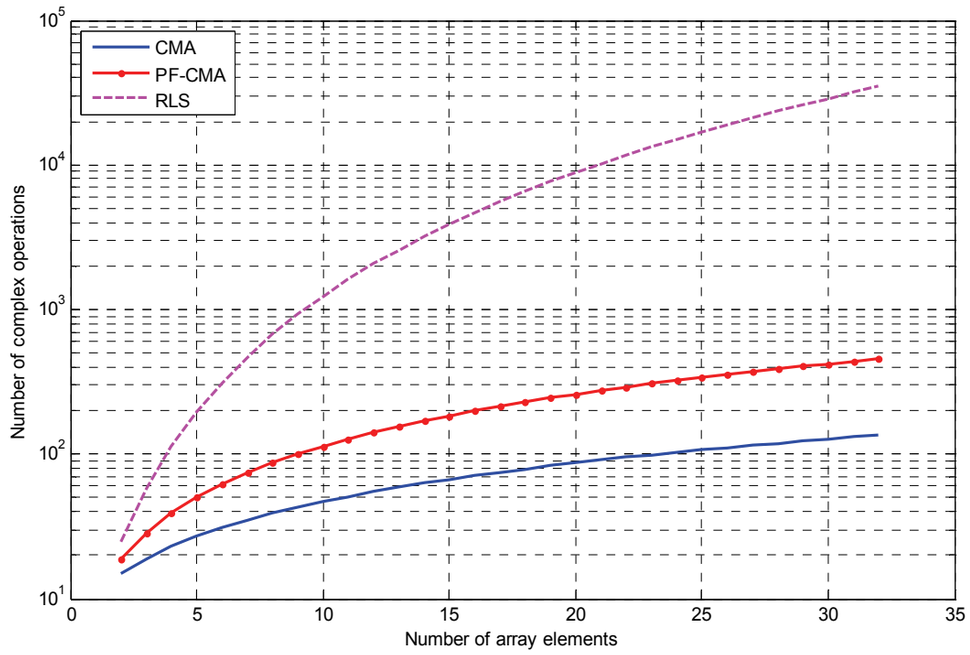


Fig. 21. Computation complexity for the hybrid algorithm and some of the conventional types of adaptive beamforming algorithms

### 4.6 Convergence speed of the proposed algorithm

Here, a comparison between the convergence speed of the conventional adaptive beamforming algorithms and the proposed hybrid technique is carried out. This speed is determined by measuring the error behavior of the algorithms versus the used samples in the training period i.e. measuring the value of the cost function (the mean square error) at each sample time. The cost functions of LMS and CMA (1, 2) algorithms are respectively as follows:

$$J_{LMS}(k) = E\left[\left|d(k) - y(k)\right|^2\right] \tag{43}$$

and

$$J_{CM(1,2)}(k) = E\left[\left|\left|y(k)\right| - 1\right|^2\right] \tag{44}$$

where $d(k)$ and $y(k)$ are the desired and output signal samples respectively. Using the same environment used for the beam pattern performance, we plotted the result of error curves in Fig. 22 by taking into account only the first significant iterations (samples) of both algorithms. From the figure it is clear that the convergence speed of the conventional algorithms is slightly faster than the hybrid technique, but this difference is very small.

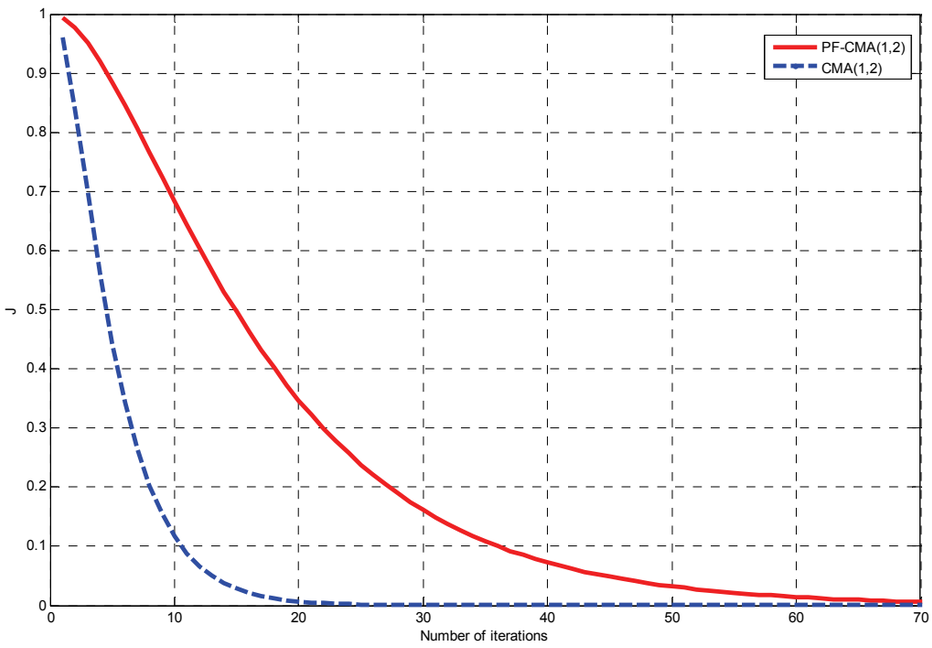


(a) Hybrid technique and CMA algorithm with $\mu = 0.001$

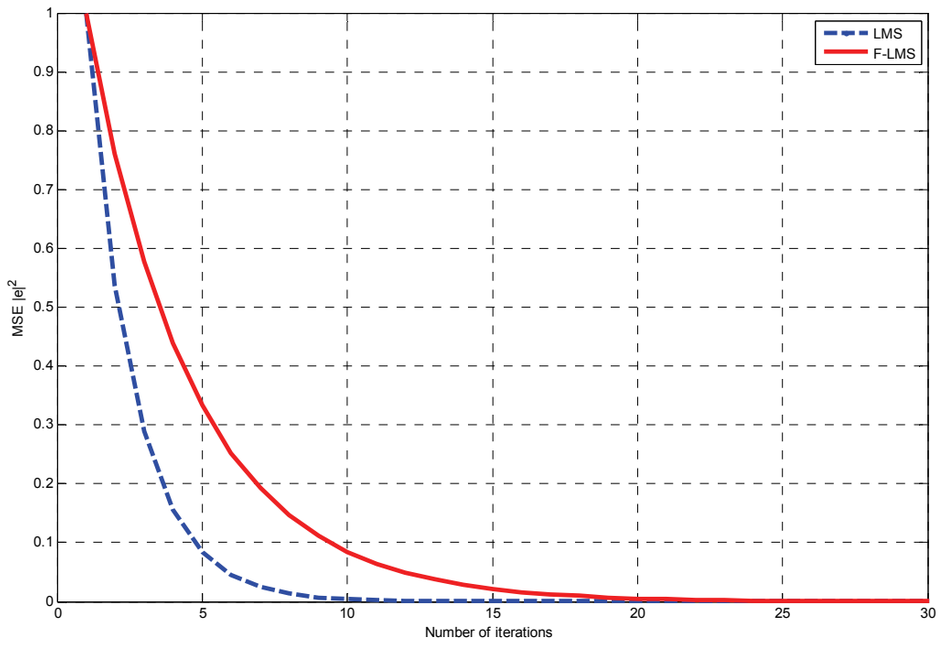


(b) LMS and hybrid LMS algorithm with $\mu = 0.001$

Fig. 22. Convergence of the hybrid and conventional algorithms

### 4.7 Tracking performances

Although the computational cost of the hybrid technique was slightly higher comparing with computational cost of the conventional technique, the simulation results have shown

that the hybrid technique is more capable of tracking the targets with varied directions of arrival. The results in Fig. 23 show that the hybrid technique can track the signal arriving from the desirable source, which has the DOA of 60˚in the initial 800 iterations; the DOA of the desired signal is changed to 30˚, where the interfering DOA remain unchanged at 0˚ in two tracking periods. We can observe that the hybrid technique is more effective in tracking

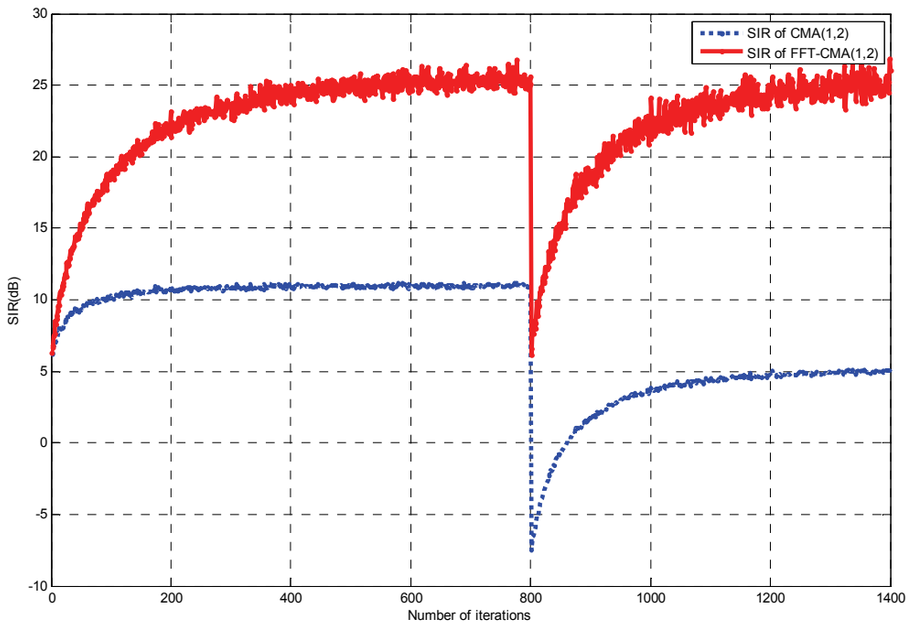


(a) Tracking from 60˚to 30˚

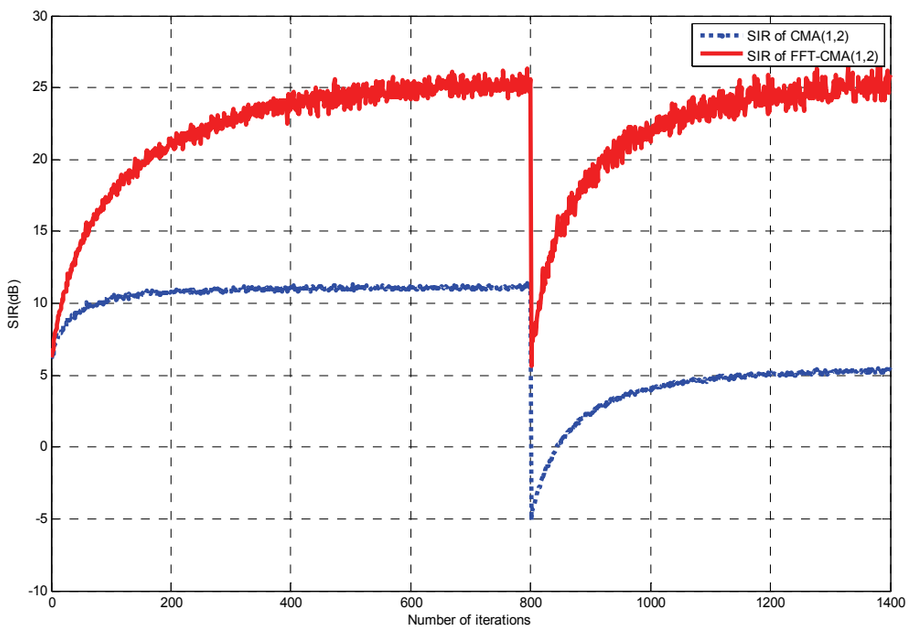


(b) Tracking from–20˚ to 60˚

Fig. 23. Tracking capabilities of the hybrid and conventional techniques References

the desired target. Also in case of the desired target is flipped to the other side of the interfering source (from –20˚ to 60˚) the hybrid tracking capability is still better than the tracking capability of the conventional technique. In fact the reason of this good tracking capability is the hybrid technique use of the initial reconstructed input signal which has less interference.

## 5. Acknowledgment

The authors express their gratitude to Professor Otman Basir, University of Waterloo, for reviewing and editing this chapter, and for his valuable remarks.

## 6. References

[1] K. Shetty, "A novel Algorithm for Up-link Interference Suppression Using Smart Antennas in Mobile Communications," A thesis submitted to the Department of Electrical and Computer Engineering, Florida State University in partial fulfillment of the requirements for the degree in Master of Science, Spring 2004.

[2] J. Litva, T. k. Lo, "Digital Beamforming in Wireless Communications," 1996.

[3] O. Abu-Ella and B. El-Jabu, "Capacity Improvement of Blind Adaptive Beamforming Algorithms Using Pre-filtering Technique," in press in IET Microwave, Antenna & Propagation Journal.

[4] Paul A. Wintz, "Transform Picture Coding," Proceedings of the IEEE, vol. 60, No. 7, July 1972.

[5] Y. Chwn, T. Le-Ngoc, B. Champagne, C. Xu, "Recursive Least Squares Constant Modulus Algorithm for Blind Adaptive Array," IEEE Transaction on Signal Processing. Vol. 52. No. 5. May 2004.

[6] A. S. Sawant, D. K. Anvekar, "Capacity Improvement in CDMA and FDMA Cellular Mobile Communication Systems Using Adaptive Antenna," 0-7803-4912-1/99, 1999 IEEE.

[7] B. El-Jabu, "Cellular Communications using Aerial Platforms," A doctoral thesis submitted in partial fulfillment of the requirements for the award of Doctor of philosophy of the university of Southampton, September 1999.


**Aerospace Technologies Advancements**

Edited by Thawar T. Arif

ISBN 978-953-7619-96-1

Hard cover, 492 pages

**Publisher** InTech

**Published online** 01, January, 2010

**Published in print edition** January, 2010

Space technology has become increasingly important after the great development and rapid progress in information and communication technology as well as the technology of space exploration. This book deals with the latest and most prominent research in space technology. The first part of the book (first six chapters) deals with the algorithms and software used in information processing, communications and control of spacecrafts. The second part (chapters 7 to 10) deals with the latest research on the space structures. The third part (chapters 11 to 14) deals with some of the latest applications in space. The fourth part (chapters 15 and 16) deals with small satellite technologies. The fifth part (chapters 17 to 20) deals with some of the latest applications in the field of aircrafts. The sixth part (chapters 21 to 25) outlines some recent research efforts in different subjects.



**InTech Europe**

University Campus STeP Ri
Slavka Krautzeka 83/A
51000 Rijeka, Croatia
Phone: +385 (51) 770 447
Fax: +385 (51) 686 166
www.intechopen.com

**InTech China**

Unit 405, Office Block, Hotel Equatorial Shanghai
No.65, Yan An Road (West), Shanghai, 200040, China
中国上海市延安西路65号上海国际贵都大饭店办公楼405单元
Phone: +86-21-62489820
Fax: +86-21-62489821

IntechOpen